A unique basaltic micrometeorite expands the inventory of solar system planetary crusts

Matthieu Gounelle[a,1], Marc Chaussidon[b], Alessandro Morbidelli[c], Jean-Alix Barrat[d], Cécile Engrand[e], Michael E. Zolensky[f], and Kevin D. McKeegan[g]

[a]Laboratoire de Minéralogie et de Cosmochimie du Muséum, Muséum National d'Histoire Naturelle, Unité Mixte de Recherche Centre National de Recherche Scientifique-7202, CP52, 57 rue Cuvier, 75005 Paris, France; [b]Centre de Recherches Pétrographiques et Géochimiques-Nancy Université-Centre National de la Recherche Scientifique, UPR 2300, 15 Rue Notre-Dame des Pauvres, France; [c]Observatoire de la Côte d'Azur, Boulevard de l'Observatoire, B.P. 4229, 06304 Nice Cedex 4, France; [d]Universite de Bretagne Occidentale-Institut Universitaire Europeen de la Mer, Centre National de la Recherche Scientifique Unité Mixte de Recherche 6538 (Domaines Océaniques), Place Nicolas Copernic, 29280 Plouzané Cedex, France; [e]Centre de Spectrométrie Nucléaire et de Spectrométrie de Masse, Centre National de la Recherche Scientifique-Université Paris-Sud, Bâtiment 104, 91 405 Orsay Campus, France; [f]SN2, National Aeronautics and Space Administration Johnson Space Center, Houston, TX 77058; and [g]Department of Earth and Space Sciences, University of California, Los Angeles, CA 90095-1567

Edited by Mark H. Thiemens, University of California at San Diego, La Jolla, CA, and approved February 20, 2009 (received for review January 13, 2009)

Micrometeorites with diameter ≈100–200 μm dominate the flux of extraterrestrial matter on Earth. The vast majority of micrometeorites are chemically, mineralogically, and isotopically related to carbonaceous chondrites, which amount to only 2.5% of meteorite falls. Here, we report the discovery of the first basaltic micrometeorite (MM40). This micrometeorite is unlike any other basalt known in the solar system as revealed by isotopic data, mineral chemistry, and trace element abundances. The discovery of a new basaltic asteroidal surface expands the solar system inventory of planetary crusts and underlines the importance of micrometeorites for sampling the asteroids' surfaces in a way complementary to meteorites, mainly because they do not suffer dynamical biases as meteorites do. The parent asteroid of MM40 has undergone extensive metamorphism, which ended no earlier than 7.9 Myr after solar system formation. Numerical simulations of dust transport dynamics suggest that MM40 might originate from one of the recently discovered basaltic asteroids that are not members of the Vesta family. The ability to retrieve such a wealth of information from this tiny (a few micrograms) sample is auspicious some years before the launch of a Mars sample return mission.

asteroids | cosmic dust | differentiation

Micrometeorites with diameter ≈100–200 μm dominate the present-day flux of extraterrestrial material reaching Earth (1). These particles are generally collected on polar ice caps in Greenland and Antarctica via ice or snow melting and filtering (2–5). Recently, large micrometeorites were also collected by magnetic sampling in the Transantarctic Mountains (6). A large majority of micrometeorites are chemically, mineralogically, and isotopically related to primitive carbonaceous chondrites (7–9), which, however, amount to only 2.5% of meteorite falls (10). This important difference between the nature of micrometeorites and that of meteorites is due to the radically different dynamical processes affecting these two kinds of objects while in interplanetary space. Meteorites are delivered on Earth via a combination of Yarkovsky thermal forces, interaction with resonances, and close encounters with the terrestrial planets (11). Micrometeorites, however, have their dynamical evolution dominated by nongravitational forces such as Poynting–Robertson drag (12), with the effects of resonances and planetary encounters playing a less important role. Therefore, micrometeorites provide a more representative sampling of solar system bodies than do meteorites (13).

Achondrites are meteorites that do not contain chondrules. Primitive achondrites have a puzzling origin (14), whereas differentiated achondrites result from the chemical differentiation of a large asteroid, a large satellite, or a planet. In addition to terrestrial (or lunar) samples, differentiated achondrites therefore provide the only samples of the planetary crusts of our solar system. Very few groups of differentiated achondrites are known (14). Lunar meteorites come from the Moon, whereas Shergottites–Nakhlites–Chassignites (SNC) meteorites are thought to originate from Mars. The Howardite–Eucrite–Diogenite (HED) meteorites as well as mesosiderites (15) are hypothesized to come from the ≈500-km, differentiated asteroid 4 Vesta (16). Angrites, aubrites, and the unique meteorite NWA011 are differentiated achondrites that have not been identified with any particular asteroid.

Although thousands of micrometeorites have been studied in detail (7), so far no unmelted micrometeorite has been found with an unambiguous achondritic composition and texture. Based purely on their chemistry, 6 totally melted micrometeorites (cosmic spherules) were tentatively linked to the HED meteorites (17) which represent the most common group of achondrites (amounting to ≈1.7% of meteorite falls). However, because cosmic spherules are fully melted during atmospheric entry (18), their original textures, mineralogy, and isotopic compositions are compromised or lost, and they cannot provide secure links to the parent bodies from which they come.

In this article, we report the discovery of a micrometeorite whose properties show that it is not related to chondrites. Despite the small size of the sample (a few micrograms), we have examined its mineralogy, its mineral chemistry, its Rare Earth Element (REE) abundance pattern, and its oxygen isotopic composition. Its magnesium isotopic composition was also investigated to detect evidence for the former presence of the short-lived radionuclide ^{26}Al ($T_{1/2}$ = 0.74 Myr) which was present in the early solar system (19).

We show that this micrometeorite is clearly a differentiated achondrite, although it is distinct from eucrites and any other achondrites group. It is a sample from a basaltic asteroid that is so far unrepresented among the meteorite collection. Numerical simulations of dust generated by known basaltic asteroids are performed to try to identify the parent asteroid of this new basaltic micrometeorite.

Mineralogy, Mineral Chemistry, and Isotopic Composition. MM40 measures 140 × 100 μm (Fig. 1) and its mass is estimated to be at most of a few micrograms, assuming a density of 3 g/cm^3. It is irregular in shape and has a granular texture. It consists of low-calcium pyroxene ($En_{29.2–47.8}Wo_{2.6–3.3}$), high-calcium pyroxene, plagioclase, SiO_2, and minor oxides and troilite (see Table 1 for the

Author contributions: M.G. designed research; M.G., M.C., A.M., J.-A.B., C.E., M.E.Z., and K.D.M. performed research; M.G., M.C., A.M., J.-A.B., C.E., M.E.Z., and K.D.M. analyzed data; and M.G. wrote the paper.

The authors declare no conflict of interest.

This article is a PNAS Direct Submission.

[1]To whom correspondence should be addressed. E-mail: gounelle@mnhn.fr.

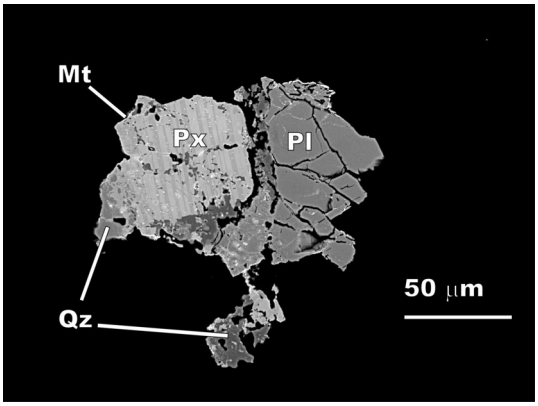

Fig. 1. Backscattered electron image of micrometeorite 99-21-40 (MM40). It consists of pyroxene (Px), plagioclase (Pl), and quartz (Qz). MM40 is covered by a thin magnetite (Mt) rim.

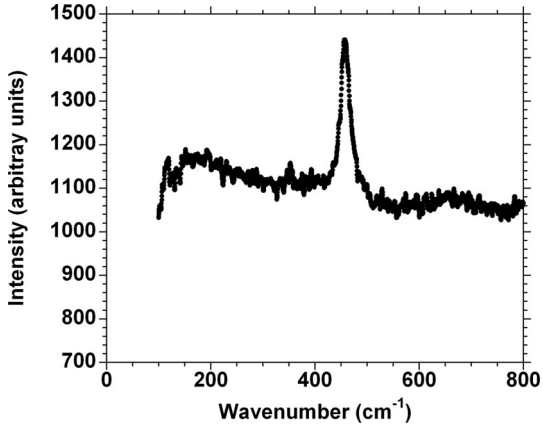

Fig. 2. Raman spectrum of the SiO_2 polymorph found in MM40. The ≈460 cm^{-1} line positively identifies it as quartz.

plagioclase and pyroxene compositions). Plagioclase has an anorthitic composition ($An_{87.1-88.9}Al_{10.8-12.6}Or_{0.28-0.45}$, average $An_{87.9}Al_{11.8}Or_{0.30}$). High-calcium pyroxene ($En_{35.6-49.0}Wo_{5.6-25.8}$, average $En_{42.8}Wo_{11.6}$) consists primarily of pigeonite with augite exsolution lamellae ranging in size from 1 to 3 μm. The pyroxene mg#, defined as the atomic ratio of Mg/(Mg+Fe), varies between 0.40 and 0.50 with an average value of 0.47. TiO_2 content in pyroxene varies between 0.20 and 0.61 wt%. SiO_2 was identified as quartz (rather than cristobalite or other polymorphs) by Raman spectroscopy (Fig. 2). It occurs as micrometer-sized inclusions within pyroxene, and also interstitial between pyroxene and plagioclase. MM40 is partially rimmed by magnetite (Fe_3O_4) also identified by using Raman spectroscopy (Fig. 3).

Both plagioclase and pyroxene have identical oxygen isotopic compositions within errors (2σ): $\delta^{18}O = 5.7 \pm 0.5$ ‰ (5.6 ± 0.6 ‰) and $\delta^{17}O = 3.4 \pm 0.3$ ‰ (3.1 ± 0.7 ‰), respectively (Fig. 4). The average $\Delta^{17}O$ for the two minerals is 0.37 ± 0.4 ‰ (2σ).

REE patterns were obtained for pyroxene and plagioclase (Fig. 5). Two pyroxene analyses display strong increases in abundances from La to Lu ($La_n/Lu_n = 0.09-0.2$, where the index n indicates normalization to CI chondrites), with pronounced negative Eu anomalies (Eu/Eu* = 0.1–0.3, where the ratio Eu/Eu* is defined as the Eu abundance normalized to the average of its two neighboring REEs, Sm and Gd, and to CI chondrites). The plagioclase pattern is flat (Fig. 5) with a moderate positive Eu anomaly (Eu/Eu* = 5.9).

Plagioclase and pyroxene have $\Delta^{26}Mg = -3.5 \pm 4.2$ ‰ and 1.5 ± 2.8 ‰, respectively. The respective Al/Mg ratios of the two minerals are 3,500 and 0. The absence of any ^{26}Mg excess even for high $^{27}Al/^{24}Mg$ ratios (Fig. 6) demonstrates that ^{26}Al was not present at the time of the Al-Mg system isotopic closure. We calculate that the upper limit of the $^{26}Al/^{27}Al$ ratio at the time of isotopic closure was of 2.8×10^{-8}.

A Unique Extraterrestrial Basalt. Given its angular shape, its texture, and its mineralogy, MM40 is undoubtedly an unmelted micrometeorite. It is not a cosmic spherule similar to those reported by ref. 17.

The texture and mineralogy of MM40 is markedly different from that of chondrites, which represent the most abundant type of meteorites falling on Earth (20). MM40 petrography and mineralogy are characteristic of basaltic rocks that result from partial melting of the mantle of rocky planets, large moons, or asteroids large enough to have undergone metal-silicate differentiation (14).

The extraterrestrial nature of MM40 is ascertained by the presence of a discontinuous magnetite rim formed during atmospheric entry (18). In addition, basalts are absent from the Terre Adélie region where the micrometeorite was collected. In

ASTRONOMY

Table 1. Pyroxene and plagioclase representative compositions (wt %)

Na_2O	MgO	Al_2O_3	SiO_2	K_2O	CaO	TiO_2	Cr_2O_3	MnO	FeO	NiO	Total
bd	12.7	0.25	49.4	bd	1.22	0.31	0.11	1.28	33.6	bd	98.9
bd	13.3	0.31	49.3	bd	2.80	0.27	0.11	1.09	30.6	bd	97.8
bd	16.1	0.22	50.7	bd	1.54	0.20	0.14	1.09	29.3	bd	99.3
bd	16.5	0.25	51.0	bd	2.63	0.26	0.09	0.99	27.2	bd	98.9
bd	14.4	0.41	49.4	bd	4.64	0.61	0.33	1.04	28.0	bd	98.8
bd	11.6	0.70	50.2	bd	11.7	0.45	0.19	0.86	22.4	bd	98.1
bd	12.8	0.23	50.0	bd	1.17	0.32	0.10	1.26	33.7	bd	99.6
bd	13.9	0.35	48.8	bd	3.54	0.30	0.11	1.10	30.1	bd	98.2
bd	15.3	0.46	50.5	bd	5.12	0.34	0.17	0.97	25.6	bd	98.5
bd	14.6	0.54	50.3	bd	7.07	0.42	0.17	0.94	24.5	bd	98.6
1.24	bd	34.7	46.8	0.04	17.5	bd	bd	bd	0.19	bd	100.7
1.15	bd	34.6	47.3	0.07	17.6	bd	bd	bd	0.22	bd	101.0
1.22	bd	33.4	45.6	0.08	16.6	bd	bd	bd	1.84	bd	98.9
1.24	bd	33.3	46.2	0.06	16.8	bd	bd	bd	0.86	bd	98.6
1.12	bd	35.0	46.7	0.07	18.1	bd	bd	bd	0.14	bd	101.2
1.16	bd	33.5	45.3	0.07	16.8	bd	bd	bd	1.77	0.06	98.9

bd, below detection limit.

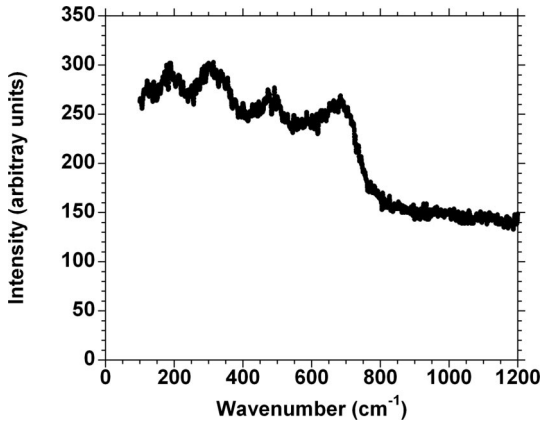

Fig. 3. Raman spectrum of the iron oxide rim of MM40. The line at ≈670 cm^{-1} unambiguously identifies magnetite (Fe_3O_4). Other lines appeared during laser excitation of the sample. They correspond to hematite (Fe_2O_3) which forms from the thermal destruction of magnetite.

the Cap Prudhomme area, the terrestrial dust component is dominated by SiO_2-rich morainic debris (21). Furthermore, major and minor elements of pyroxene in MM40 are radically different from those of Antarctic basalts such as from Mount Erebus (22), excluding the possibility that MM40 was transported from the Transantarctic Mountains to the Terre Adélie. Finally, the average Fe/Mn ratio of pyroxene is 26.5 ± 0.6, significantly lower that the terrestrial value, Fe/Mn = 40 ± 11 (23).

The mineralogy of MM40, dominated by pyroxene and anorthite, is reminiscent of that of eucrites (formerly named pyroxene-plagioclase achondrites), of the unique achondrite NWA011, and of some silicate clasts in mesosiderites (14). It is significantly different from angrites and martian meteorites (14). It is also radically different from differentiated, plagioclase-bearing clasts found in ordinary chondrites (24–26). These clasts found in Tieschitz (H/L 3.6), Manych (LL3.4), and Bovedy (L3) have less calcic and more sodic plagioclase compositions ($An_{80-85}Al_{16-19}$) than MM40 ($An_{88}Al_{12}$). Low-calcium pyroxenes from these clasts have compositions far more magnesia-rich (En_{72-88}) than MM40 (En_{39-48}). Finally, these clasts contain abundant olivine (24–26) which is absent from MM40.

The pyroxene Fe/Mn ratio has long been known as a good discriminator of the different sources of solar system basalts (23). The Fe/Mn ratio of pyroxene from MM40 (26.5 ± 0.6) is markedly lower than that of lunar basalts (62 ± 18) or angrites (111 ± 23) and marginally lower than pyroxenes in HED meteorites (30 ± 2) or SNC (martian) meteorites (32 ± 6) (23).

The oxygen isotopic composition ($\delta^{18}O$ and $\Delta^{17}O$ values) of micrometeorite MM40 is compatible only with lunar samples, and marginally with SNC (martian) meteorites (Fig. 4). Compared with eucrites and other meteorites coming from (4) Vesta, MM40 has significantly heavier $\delta^{18}O$ values (Fig. 4). Note that any reequilibration of oxygen isotopes with Antarctic ice would

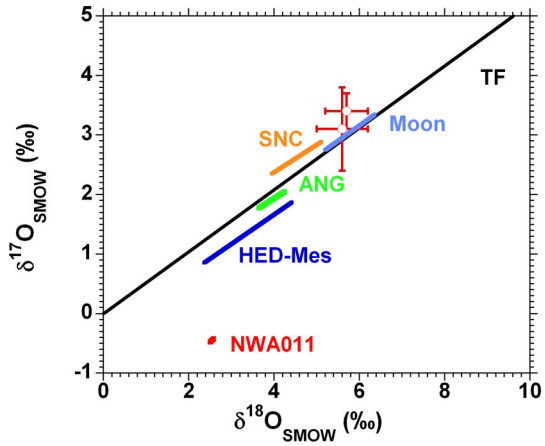

Fig. 4. Oxygen isotopic composition of MM40 (open red circles) compared with that of other extraterrestrial basalts. Data from refs. 45–47. ANG, HED, and Mes stand, respectively, for angrites, howardites-eucrites-diogenites, mesosiderites.

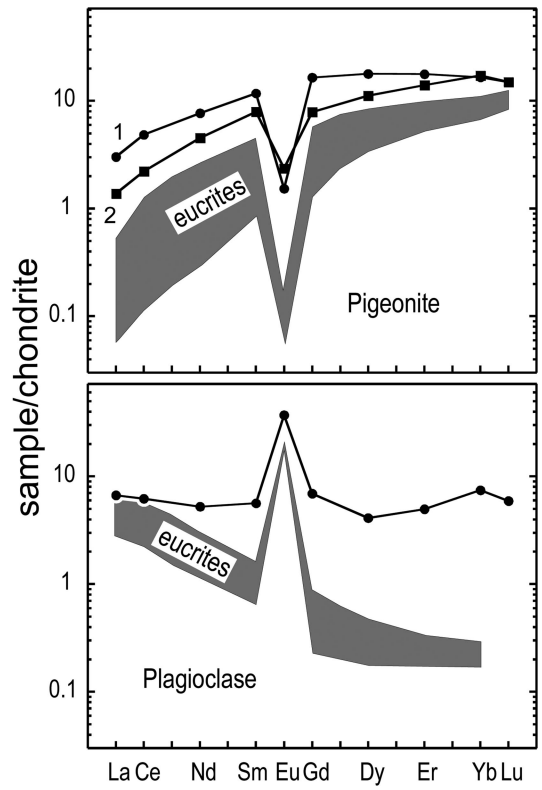

Fig. 5. CI normalized REE patterns for pyroxene and plagioclase from MM40. The shaded regions show the range of REE abundances observed in plagioclase and pigeonite from highly metamorphosed basaltic eucrites (28).

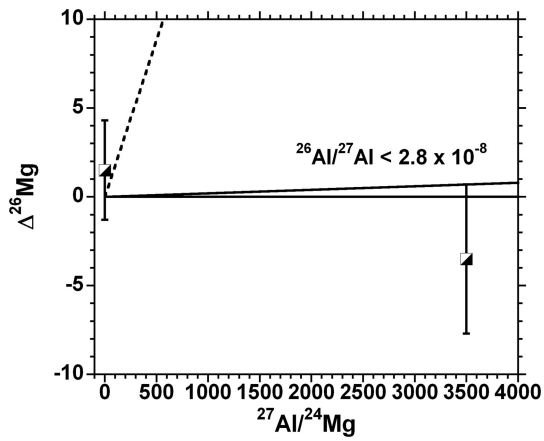

Fig. 6. Al-Mg isochron diagram for pyroxene (low Al/Mg ratio) and plagioclase (high Al/Mg ratio) in MM40. The $^{26}Al/^{27}Al = 4.5 \times 10^{-5}$ (dashed) and $^{26}Al/^{27}Al = 2.8 \times 10^{-8}$ (solid) lines are shown for reference.

have lead to a decrease of $\delta^{18}O$, compromising further the relationship with eucrites (27).

The REE patterns (Fig. 5) are approximately similar to those obtained for pigeonite from eucrites (28, 29), but both pyroxene analyses show higher REE concentrations than pigeonites from eucrites. The flatness of the plagioclase REE pattern and the moderate europium enrichment (Eu/Eu* = 5.9) contrasts with eucritic plagioclase grains, which have markedly light REE enrichments, much lower heavy REE abundances, and higher Eu/Eu* ratios. It is unlikely that these differences are due to plagioclase contamination by REE-rich phases such as phosphate or zircon because an unrealistically large amount of these minerals would be necessary to (partially) explain the differences between MM40 plagioclase and eucritic plagioclase. Specifically, the addition of zircon or phosphate would not erase the initial light REE enrichment of MM40 plagioclase. The distinctive REE pattern of MM40 plagioclase supports the conclusion, based on mineral chemistry and oxygen isotopic composition, that MM40 is not related to eucrites.

Because its isotopic composition, mineral chemistry, and trace element abundances do not match any basalt either from Mars, the Moon (4), Vesta, or the angrite parent body, we conclude that MM40 is a basaltic rock originating from a hitherto unsampled large asteroid or a planet. Because it does not come from Mars, and because it is dynamically very unlikely that it originates from Mercury or Venus (see below), it is a unique extraterrestrial basalt of asteroidal origin.

Basaltic Dust Dynamics. Venus can be excluded as a reasonable source for MM40 because this planet is comparable in mass to the Earth, and thus only very large impacts can strip meteorites as well as micrometeorites from that planet. In addition, the large Venusian atmosphere would also jeopardize any launch of meteorites and micrometeorites. It has recently been shown that, given the small size of Mercury, meteorites and micrometeorites from that planet can be emplaced directly in orbits with an aphelion distance >1 AU (30). However, although Mercurian dust could in principle be transported to Earth, no space mission has ever detected Mercury as a significant dust source. In addition, Infrared Astronomical Satellite (IRAS) data do not indicate any Mercurian (or Venusian) component. In conclusion, it is unlikely MM40 originates from the two inner planets.

Numerical investigation of the dynamics of dust generated by basaltic asteroids can help constrain the source of MM40. In addition to the members of the Vesta family, several other basaltic asteroids (non-Vestoids hereafter) have now been identified (31–33). A few of them, such as (1459) Magnya, are in the outer main belt beyond 2.8 AU (5:2 resonance with Jupiter). Several others, like (21238) 1995 WV7 and (40521) 1999 RL95, are located in the central belt beyond 2.5 AU (3:1 resonance with Jupiter). The majority are located inside 2.5 AU. Among these, some might be fugitives from the Vesta family but others, like (4796) Lewis and (5379) Abehiroshi, have too low of an inclination, so that, if they are genetically linked to Vesta, they must have been ejected from it before the Late Heavy Bombardment period (3.8 Gy ago) as recently shown by ref. 33.

We performed orbital integrations of particles of 120 μm in diameter, and bulk density of 3 g/cm^3, launched by the asteroids quoted above. The trajectories of 50 particles from each asteroid were calculated. We accounted for the gravitational perturbations exerted by the planets and for the Poynting–Robertson effect that causes small particles to drift toward the Sun on a 10^5 yr timescale. Particles were discarded when they hit a planet, the Sun, or were ejected from the solar system. Otherwise the simulations covered a time span of 2 Myr.

From the time evolution of the orbital elements of these particles, the mean collision probability and the mean collision velocity (accounting for Earth's focusing factor) were calculated.

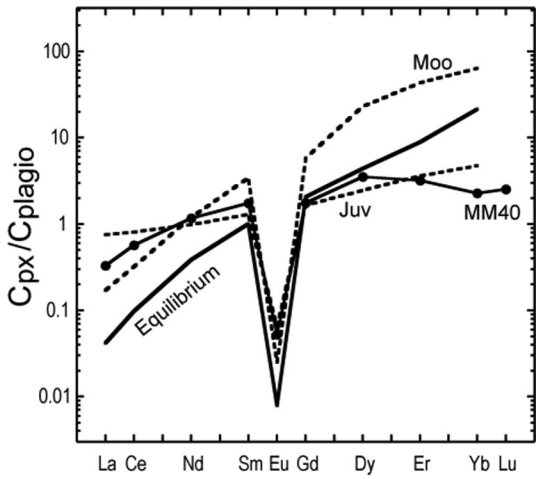

Fig. 7. Apparent partition coefficient between pyroxene and plagioclase for MM40 (this study), the eucrites Moore County and Juvinas (48). The equilibrium values are shown for comparison.

We found that particles released by (4796) Lewis (5379) Abehiroshi, (21238) 1995 WV7, and (4) Vesta have on average a probability for collision with the Earth varying between 2.7×10^{-3} and 3.6×10^{-3}, with a mean impact velocity of 12.4 km/s. (40521) 1999 RL95 has a lower collision probability (1.8×10^{-3}) and a higher mean impact velocity (14.0 km/s), similar to those from (1459) Magnya (1.1×10^{-3} and 4.3 km/s). The differences between these two groups of objects can be understood in terms of the orbital inclinations of the parent bodies and the number of strong resonances that the particles have to cross before reaching the Earth.

The collision probabilities and impact velocities of the particles coming from all of these parent asteroids are similar enough that we cannot favor or disregard any of these sources, except maybe (40521) 1999 RL95 and (1459) Magnya. These asteroids are more unlikely sources of MM40 because of their lower collision probability *and* their higher impact velocity, which would compromise the atmospheric entry of MM40 without melting.

Interestingly, the discovery of the first recognized basaltic micrometeorite might shed light on the origin of basaltic asteroids. Debiasing the orbital and size distribution of the non-Vestoids basaltic candidates, it was found that 60% of them are inside 2.5 AU (34). Thus, if the non-Vestoids inside 2.5 AU were mostly genetically linked to (4) Vesta as mentioned above, it would be unlikely that the first recognized basaltic micrometeorite (MM40) is not linked (on petrographic and geochemical grounds) to that asteroid. Instead, if the non-Vestoids are fragments of different parent bodies from the terrestrial planets region, the odds for sampling a distinct basaltic micrometeorite like MM40 are more favorable. In fact, it was estimated that the total mass of all non-Vestoid objects is about the same of that of the Vesta family members [(4) Vesta excluded] (34). Thus, we conclude that the discovery of MM40 and its petrographic as well as its geochemical properties support the hypothesis that (4796) Lewis, (5379) Abehiroshi, their fellow asteroids, as well as (40521) 1999 RL95 are not related to the Vesta family.

Thermal Metamorphism on MM40's Parent Asteroid. As for most basaltic achondrites, the composition of the parental melt of MM40 cannot be directly derived from the REE abundances (35). The distribution of REE abundances between plagioclase and pyroxene is far from magmatic values (Fig. 7). These differences are interpreted as a sign of intense thermal metamorphism, as well as the augite exsolution within pigeonite and

the relatively homogeneous composition of pyroxenes. Applying a scheme developed for eucrites, MM40 would be placed among equilibrated rocks of petrographic type >4 (36), indicative again of significant thermal metamorphism.

Aluminium-26 is a short-lived radionuclide that decays to ^{26}Mg with a half-life of 0.74 Myr. It was present in the early solar system at an initial abundance of $^{26}Al/^{27}Al \approx 4.5 \times 10^{-5}$ (19) and thus early crystallized Al-bearing minerals are expected to contain ^{26}Mg excesses due to ^{26}Al decay (37). However, no ^{26}Mg excesses were detected in MM40 plagioclase, providing an upper limit of the $^{26}Al/^{27}Al$ ratio at the time of isotopic closure of 2.8×10^{-8}. Assuming that ^{26}Al was homogeneously distributed in the early solar system and thus can serve as a relative chronometer (see ref. 38 for an alternative view), this indicates that thermal metamorphism on MM40 parent body ended no earlier than 7.9 Myr after solar system formation.

Thermal metamorphism can be due either to protracted thermal activity (due to differentiation) or to impact cratering (39). The larger an asteroid is, the longer its thermal activity lasts (40). The parent asteroid of MM40 is smaller than (4) Vesta, which is the largest differentiated asteroid. Therefore, if thermal activity due to differentiation was the main source of thermal metamorphism, one would expect to find some indication of ^{26}Al in MM40, given that some ^{26}Al was present in eucrites (37), which are thought to derive from (4) Vesta. The absence of ^{26}Al in MM40 implies that impact cratering is a more likely source for MM40 parent-body metamorphism than protracted thermal activity. In that respect, it is interesting to have identified quartz as the SiO_2 polymorph. The presence of quartz together with the absence of coesite/stishovite shows that MM40 was little shocked (41), with a shock pressure probably below a few Gpa (42), demonstrating that metamorphism due to impact can extend far away from the shock region.

Materials and Methods

Micrometeorite 99-21-40 (hereafter, MM40) was collected in the blue ice fields of Cap Prudhomme (Terre Adélie, Antarctica) in 1994 by Michel Maurette and collaborators (43). It was embedded in epoxy EMBED 812 and polished following the standard procedures at Orsay (7). Preliminary examination was made by using scanning electron microscopy at the Naturhistoriches Museum in Wien.

Scanning electron microscopy (SEM) was performed at the Service Commun de Microscopie (CAMPARIS – Université Paris 6) by using a JEOL 840 SEM equipped with an energy-dispersive X-ray (EDX) detector which provided qualitative mineral compositions. Quantitative mineral compositions were obtained at CAMPARIS with a CAMECA SX100 Electron Microprobe (EMP) operated at a 15 kV acceleration voltage and a 10 nA current. Detection limits of all oxides are ≈0.02 wt %. Longer counting times (30 s) were used for manganese to improve precision on the determination of the Fe/Mn ratio.

Raman spectroscopy was used to distinguish between several mineral polymorphs. Minerals were excited at a wavelength of 632.8 nm with a Jobin Yvon Horiba Labram laser Raman microprobe at Johnson Space Center (Houston, TX). Filters and rastered-beam scans were used to minimize sample heating.

The oxygen isotopic compositions of plagioclase and pyroxene were determined by using the Cameca ims 1270 ion microprobe at Centre de Recherches Pétrographiques et Géochimiques (CRPG)-Centre National de la Recherche Scientifique (Nancy, France) following the procedures previously described (44). The three oxygen isotopes were measured in multicollection mode (using a Faraday cup for ^{16}O and two electron multipliers for ^{17}O and ^{18}O) with a primary Cs^+ ion beam of 5–10μm size and 0.2 nA intensity. Two terrestrial standards were used to determine instrumental mass fractionation: an orthopyroxene from a mantle xenolith (Vitim 313–3, $\delta^{18}O = +5.8‰$) for pyroxene and a volcanic glass of acidic composition (Macusani JV1, $\delta^{18}O = +12.2‰$) for plagioclase. The deviation from the terrestrial mass fractionation line, named $\Delta^{17}O$, was calculated according to the equation $\Delta^{17}O = \delta^{17}O - 0.52 \times \delta^{18}O$. The two sigma external reproducibility for $\delta^{17}O$, $\delta^{18}O$, and $\Delta^{17}O$ on the standards was equal to ±0.28‰, ±0.50‰, and ± 0.36‰, respectively (9 analyses). The two sigma errors given in the text are calculated for each point by adding in quadratic fashion the two sigma internal error (counting statistics) to the two sigma external reproducibility (as determined from the analyses of standards).

The REE (La, Ce, Nd, Sm, Eu, Gd, Dy, Er, Yb, and Lu) abundances were measured on a Cameca ion microprobe IMS 3f at CRPG-Centre National de la Recherche Scientifique, Nancy, France. A primary beam of negative oxygen ions (≈ 25 nA) was focused to a size of ≈30 μm. An offset of −80 eV was applied through a 25 eV energy window. The positive secondary ion intensities were measured with an electron multiplier integrated >10 s and repeated >15 cycles. Ratios of the REE to ^{30}Si intensity were determined as a function of the known content in REE for each reference material used in this study. The average external error determined by repeated measurements on reference material was 5–10%.

The Mg isotopic composition was measured with the University of California, Los Angeles, Cameca ims 1270 ion microprobe using an oxygen primary beam, with a beam size of ≈20 μm in aperture illumination mode. The three isotopes of Mg were counted on an electron multiplier in monocollection (peak-jumping) mode. The mass resolving power was set ≈4,200 to resolve all molecular ion interferences. Data were corrected for deadtime and instrumental mass fractionation by using Madagascar hibonite as a standard. The $Al/^{24}Mg$ of each measured spot was determined from the ion ratios $Al^+/^{24}Mg^+$ by employing a relative sensitivity factor determined from analyses of standards (Madagascar hibonite and synthetic glass of plagioclase composition) made under the same analytical conditions. Data are reported as $\Delta^{26}Mg = \delta^{26}Mg - 2 \times \delta^{25}Mg$, where $\delta^i Mg = 1{,}000 \times ({}^iMg/{}^{24}Mg)_{sample}/({}^iMg/{}^{24}Mg)_{ref}$ with i = 26 or 25, $({}^{25}Mg/{}^{24}Mg)_{ref} = 0.12663$, and $({}^{26}Mg/{}^{24}Mg)_{ref} = 0.13932$ (e.g., 19).

ACKNOWLEDGMENTS. We thank Michel Maurette and Gero Kurat for their pioneering work on micrometeorites and for fruitful discussions and insights on the origin of this particle, and two anonymous reviewers for their very constructive comments, and for bringing our attention to the basaltic clasts in ordinary chondrites. This work was supported by the Program National de Planétologie (PNP), the France-États-Unis fund from Centre National de la Recherche Scientifique [2006-3482], and European Grant ORIGINS [MRTN-CT-2006-035519]. The Institut Polaire Français Paul-Emile Victor (IPEV) constantly supported the efforts of the Orsay group to collect micrometeorites. This is CRPG contribution #1989.

1. Love SG, Brownlee DE (1993) A direct measurement of the terrestrial mass accretion rate of cosmic dust. *Science* 262:550–553.
2. Duprat J, et al. (2007) Micrometeorites from central Antarctica snow: The CONCORDIA collection. *Adv Space Res* 39:605–611.
3. Taylor S, Lever JH, Harvey RP (1998) Accretion rate of cosmic spherules measured at South Pole. *Science* 392:899–903.
4. Maurette M, et al. (1991) A collection of diverse micrometeorites recovered from 100 tons of Antarctic blue ice. *Nature* 351:44–47.
5. Nakamura T, et al. (1999) Antarctic micrometeorites collected at the Dome Fuji Station. *Antarct Meteorite Res* 12:183–198.
6. Rochette P, et al. (2008) Micrometeorites from the Transantarctic Mountains. *Proc Natl Acad Sci USA* 105:18206–18211.
7. Engrand C, Maurette M (1998) Carbonaceous micrometeorites from Antarctica. *Meteoritics Planet Sci* 33:565–580.
8. Gounelle M, et al. (2005) Small Antarctic micrometeorites (25–50 μm): A mineralogical and in situ oxygen isotopes study. *Meteoritics Planet Sci* 40:917–932.
9. Genge MJ, et al. (2008) The classification of micrometeorites. *Meteoritics Planet Sci* 43:497–515.
10. Grady MM (2000) *Catalogue of Meteorites* (Cambridge Univ Press, Cambridge, UK).
11. Vokrouhlický D, Farinella P (2000) Efficient delivery of meteorites to the Earth from a wide range of asteroid parent bodies. *Nature* 407:606–608.
12. Burns JA, Lamy PL, Soter S (1979) Radiation forces on small particles in the Solar System. *Icarus* 40:1–48.
13. Genge MJ, Grady MM, Hutchison RH (1997) The textures and compositions of fine-grained micrometeorites: Implications for comparisons with meteorites. *Geochim Cosmochim Acta* 61:5149–5162.
14. Mittlefehldt DW, et al. (1998) Non-chondritic meteorites from asteroidal bodies. *Planetary Materials*, ed Papike JJ (Mineralogical Society of America, Washington, DC), Vol 36, pp 4.01–4.195.
15. Greenwood RC, et al. (2006) Oxygen isotope variation in stony-iron meteorites. *Science* 313:1763–1765.
16. Binzel RP, Xu S (1993) Chips off of Asteroid 4 Vesta: Evidence for the parent body of basaltic achondrite meteorites. *Science* 260:186–191.
17. Taylor S, Herzog GF, Delaney JS (2007) Crumbs from the crust of Vesta: Achondritic cosmic spherules from the South Pole water well. *Meteoritics Planet Sci* 42:223–233.
18. Toppani A, et al. (2001) Experimental simulation of atmospheric entry of micrometeorites. *Meteoritics Planet Sci* 36:1377–1396.
19. MacPherson GJ, Davis AM, Zinner EK (1995) The distribution of aluminum-26 in the early Solar System: A reappraisal. *Meteoritics* 30:365–386.
20. Brearley AJ, Jones RH (1998) Chondritic meteorites. *Planetary Materials*, ed Papike JJ (Mineralogical Society of America, Washington, DC), Vol 36, pp 3.1–3.398.

21. Kurat G, et al. (1995) On the terrestrial dust component in the ice at Cap Prudhomme, Antarctica. *Abstr Lunar Planet Sci Conf* 26:811–812.
22. Kyle PR, Moore JA, Thirwall MF (1992) Petrologic evolution of anorthoclase phonolite lavas at Mount Erebus, Ross Island, Antarctica. *J Petrol* 33:849–875.
23. Papike JJ, Karner JM, Shearer CK (2003) Determination of planetary basalt parentage: A simple technique using the electron microprobe. *Am Mineral* 88:469–472.
24. Grossman JN, Rubin AE (1986) The origin of chondrules and clasts bearing calcic plagioclase in ordinary chondrites. *Abstr Lunar Planet Sci Conf* 17:293–294.
25. Hutchison R, Graham AL (1975) Significance of calcium-rich differentiates in chondritic meteorites. *Nature* 255:471.
26. Hutchison R (1982) Meteorites—Evidence for the interrelationships of materials in the solar system of 4.55 Ga ago. *Phys Earth Planet Interiors* 29:199–208.
27. Bland PA, et al. (2000) Aqueous alteration without a pronounced oxygen-isotopic shift: Implications for the asteroidal processing of chondritic material. *Meteoritics Planet Sci* 35:1387–1395.
28. Floss C, et al. (2000) Trace element constraints on the origins of highly metamorphosed Antarctic eucrites. *Antarct Meteorite Res* 13:222–237.
29. Hsu W, Crozaz G (1996) Mineral chemistry and the petrogenesis of eucrites: I. Noncumulate eucrites. *Geochim Cosmochim Acta* 60:4571–4591.
30. Gladman B, Coffey J (2008) Mercurian impact ejecta: Meteorites and mantle. *Asteroids, Comets, Meteors*, no. 9289.
31. Sunshine JM, et al. (2004) High-calcium pyroxene as an indicator of igneous differentiation in asteroids and meteorites. *Meteoritics Planet Sci* 39:1343–1357.
32. Roig F, et al. (2008) V-type asteroids in the middle main belt. *Icarus* 194:125–136.
33. Nesvorný D, et al. (2008) Fugitives from the Vesta family. *Icarus* 193:85–95.
34. Moskovitz NA, et al. (2008) The distribution of basaltic asteroids in the Main Belt. *Icarus* 198:77–90.
35. Treiman AH (1996) The perils of partition: Difficulties in retrieving magma compositions from chemically equilibrated basaltic meteorites. *Geochim Cosmochim Acta* 60 147–155.
36. Takeda H, Graham AL (1991) Degree of equilibration of eucritic pyroxenes and thermal metamorphism of the earliest planetary crust. *Meteoritics* 26:129–134.
37. Srinisavan G, Goswami JN, Bhandari N (1999) ^{26}Al in Eucrite Piplia Kalan: Plausible heat source and formation chronology. *Science* 284:1348–1350.
38. Gounelle M, Russell SS (2005) On early Solar System chronology: Implications of an heterogeneous distribution of extinct short-lived radionuclides. *Geochim Cosmochim Acta* 69:3129–3144.
39. Yamaguchi A, Taylor GJ, Keil K (1996) Global crustal metamorphism of the eucrite parent body. *Icarus* 124:97–112.
40. Ghosh A, McSween HY Jr (1998) A thermal model for the differentiation of asteroid 4 Vesta, based on radiogenic heating. *Icarus* 134:187–206.
41. Chennaoui Aoudjehane H, Jambon A (2007) Determination of silica polymorphs by cathodoluminescence (abstract). *Abstr Lunar Planet Sci Conf* 38:1714.
42. Férrière L, Koeberl C, Reimold WU (2009) Characterisation of ballen quartz and cristobalite in impact breccias: New observations and constraints on ballen formation. *Eur J Mineral* 21:203–217.
43. Maurette M, et al. (1994) The 1994 EUROMET collection of micrometeorites at Cap-Prudhomme, Antarctica (abstract). *Meteoritics* 29:499.
44. Chaussidon M, Libourel G, Krot AN (2008) Oxygen isotopic constraints on the origin of magnesian chondrules and on the gaseous reservoirs in the early solar system. *Geochim Cosmochim Acta* 72:1924–1938.
45. Clayton RN (1993) Oxygen isotopes in meteorites. *Annual Review of Earth and Planetary Sciences* 21:115–149.
46. Franchi IA (2008) Oxygen isotopes in asteroidal materials. *Rev Mineral Geochem* 68:345–397.
47. Yamaguchi A, et al. (2003) A new source of basaltic meteorites inferred from Northwest Africa 011. *Science* 296:334–336.
48. Schnetzler CC, Philpotts JA (1969) Genesis of the calcium-rich achondrites in light of rare-earth and barium concentrations. *Meteorite Research*, ed Millman PM (Reidel, D., Dordrecht, The Netherlands), pp 206–216.